IOP Conference Series: Materials
Science and Engineering

PAPER • OPEN ACCESS

Impact of sand feed rate on the damage of railway wheel steels

To cite this article: N Zani *et al* 2024 *IOP Conf. Ser.: Mater. Sci. Eng.* **1306** 012036

View the article online for updates and enhancements.

Impact of sand feed rate on the damage of railway wheel steels

N Zani[1,*], K Shu[2], L Ghidini[1], C Petrogalli[1] and A Mazzù[1]

[1] Department of Mechanical and Industrial Engineering, University of Brescia, Brescia, 25123, Italy
[2] College of Mechanical Engineering, Hunan Institute of Science and Technology, Yueyang, 414006, China

* E-mail: nicola.zani@unibs.it

Abstract. The global railway industry plays a pivotal role in economic development, offering efficient transportation solutions. However, railways operating in desert environments face unique challenges due to windblown sand. This study investigates the influence of sand feed rates on wheel-rail wear in desert conditions. Experimental tests were conducted using a bidisc apparatus to simulate sand feed rates. Results indicate that low feed rates lead to spalling and pitting, while high rates increase abrasive and fatigue wear. A critical transition point at 0.4 g/min suggests sand-induced abrasion of wheel surfaces. Moreover, the research highlights the crucial role of sand feed rates not only in wear but also in surface roughness, further emphasizing the complex interplay between sand transport rates, adhesion, and wear mechanisms. These insights provide valuable guidance for mitigating wear-related challenges in desert railway operations and optimizing maintenance strategies.

1. Introduction

The global railway industry has played a pivotal role in driving industrialisation and economic development for well over a century. Railway networks have provided unmatched advantages, such as substantial transportation capacity, cost-efficiency, energy conservation, environmental sustainability, and safety. This enduring legacy has led to continual expansion, resulting in the establishment of extensive railway networks. Among the challenging environmental conditions and extreme landscapes, deserts stand out as the most significant technical challenge that new railways must address.

A significant concern in these regions is the pronounced damage and wear experienced by railway materials, surpassing what is observed in dry environments [1–4]. The gravity of this issue often becomes evident only after extended periods of service. This complexity arises from the dynamic and multifaceted nature of windblown sand environments, subject to constant changes driven by factors such as landform features and weather fluctuations. Furthermore, various factors, including the accumulation of sand on rail surfaces following sandstorms, issues affecting rail ballast due to dynamic windblown sand phenomena and sand infiltration can influence the wear and tear on wheels and rails.

A particular area of research has been dedicated to studying the influence of sand feed rate on wear, damage, and adhesion at the interface between the railway wheel and rail. Several papers showed that, when there is no liquid lubricant at the contact interface, the increase of sand feed rate has been associated with decreasing adhesion, primarily due to solid lubrication effects [2,4–10]. This phenomenon is caused by sand, which notably reduces the overall friction coefficient by reducing tangential forces. This reduction results from both the separation of wheel and rail surfaces and the sand grains' rolling motion.

Experiments conducted using small-scale bidisc apparatus have elucidated that the sand feed rate notably affects damage patterns and wear regimes. Under conditions of low sand feed rates (up to approximately 2.5 g/min) [6,9], predominant surface damage phenomena manifest as spalling and pitting, with the former exhibiting decreased prominence as transport rate conditions escalate. It is crucial to emphasise that slow feeding rates are directly linked to adhesive and oxidative wear. The acceleration of black oxide formation is attributed to an augmented quantity of pits induced by sand particles infiltrating the wheel-rail interface. Noteworthy findings include cross-sectional analyses revealing a thin oxide layer hosting entrapped sand particles within.

Conversely, higher sand feed rates are unequivocally correlated with escalated wear rates for both rail and wheel materials, regardless of adhesion conditions [2]. The wear mechanisms observed encompass abrasive and fatigue phenomena [1.11], resulting in a surface layer characterised by pronounced ratcheting due to the presence of sand fragments and wear debris, as well as a subsurface layer exhibiting less severe plastic deformation [2,12–13]. It is essential to highlight that these damage features become significantly more pronounced as sand feeding rates increase, emphasising the complex interplay between sand, adhesion, and wear mechanisms [14]. Moreover, the influence of sand extends beyond the realms of adhesion and wear, introducing erosive wear. This adds an additional layer of complexity to the dynamic interplay. As such, it is imperative to comprehensively examine how sand transport rates exert influence over wheel and rail wear and damage in windblown sand environments.

This work embarks on an exhaustive exploration of these challenges within the context of desert windblown sand environments. This study seeks to closely examine how varying rates of sand feed rate impact the damage characteristics and wear of the materials. We will achieve this objective by employing a two-disc testing machine. Our aim is to clarify the points where the shift occurs between oxidative and abrasive wear patterns.

2. Experimental setup

The experimental tests described here were carried out using an advanced bi-disc apparatus with high performance capabilities. Figure 1 provides an illustration of the setup used in these experiments. The apparatus was equipped with two mandrels, one of which could move along linear slides. These mandrels were powered by two separate alternating current motors (33 kW), capable of achieving speeds of up to 1200 rpm. A servo-hydraulic actuator with a capacity of 75 kN was employed to apply the contact load. Information regarding the normal load and torque was gathered at a frequency of 5 Hz using a data acquisition system from National Instruments.

The cylindrical test specimens were manufactured from the railhead and wheel-tread surfaces, with a thickness of 15 mm and a diameter of 60 mm. Given their cylindrical shape, the contact track width matched the specimen thickness. In this work, the wheel and rail steels chosen were UNI EN ER8 and 900A, respectively. Their mechanical properties and chemical compositions are listed in Table 1. The tests were carried out under the theoretical Hertzian pressure (1100 MPa), creepage (0.0314 m/s) and average rolling speed (500 r.p.m.). All the tests were performed for 40×10^4 cycles. The experiments were conducted under both clean and solid contaminated conditions. Silica sand was used in these tests; the primary component of the sand is SiO_2. The maximum granulometry of the particles was 0.500 mm. The tested sand feed rate ere 0 (clean condition), 0.1, 0.2, 0.4, 1 and 3 g/min.

During the tests, the friction coefficient of every test was determined from torque measurement. After the experiments, the samples were ultrasonically cleaned and weighed by a precision balance with a resolution of 0.001 g and the mass loss was calculated. The surface analysis was used by a laser scanning confocal microscope (LSCM, OLS5000-SAF, Japan) and a scanning electron microscope (SEM, TESCAN MIRA LMS, Czech Republic) equipped with an energy disperse spectroscopy (EDS). The wheel samples were also sectioned along the mid plane orthogonally to their axis; the section was ground, polished and etched with 2% Nital and examined with a LEICA DM6000M light optical microscope.

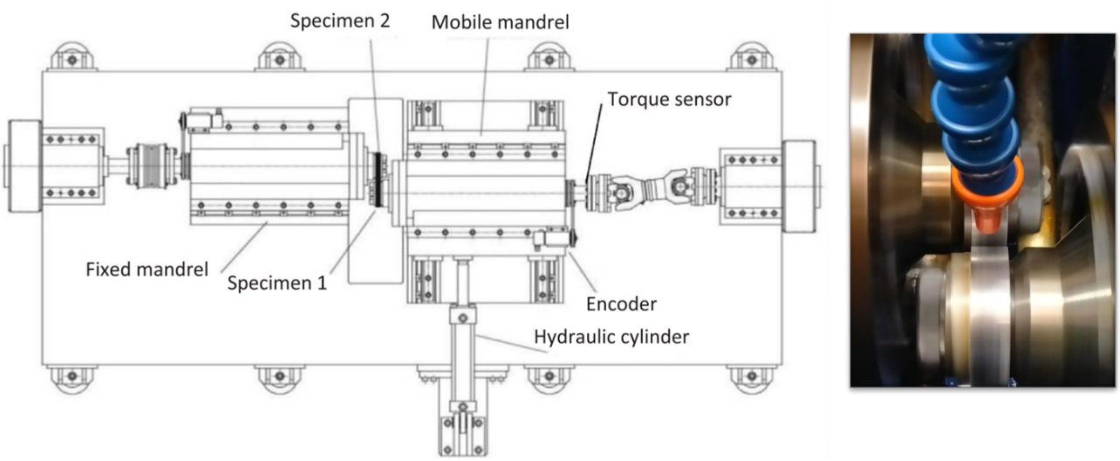

Figure 1 – Bi-disc testing machine.

Table 1 – Mechanical properties and chemical composition of the samples' steels.

		ER8	**900 A**
Chemical composition [wt%]	**C**	0.52	0.71
	Mn	0.74	1.07
	Cr	0.22	0.03
	Ni	0.16	0.02
	Mo	0.031	0.01
	Si	0.37	0.27
Ultimate tensile strength [MPa]		940	930
Yield strength [MPa]		590	470
Elongation [%]		17	14
Vickers hardness		298	263

3. Results

3.1. Friction coefficient and wear rate

The experimental friction coefficient was calculated by dividing the measured torque by the normal load and the sample's radius. Figure 2 shows the stabilised friction coefficients according to the sand feed rates. Compared to the value around 0.55 under clean conditions, the friction coefficient shows a descending trend to about 0.21 under the highest tested feed rate (3 g/min).

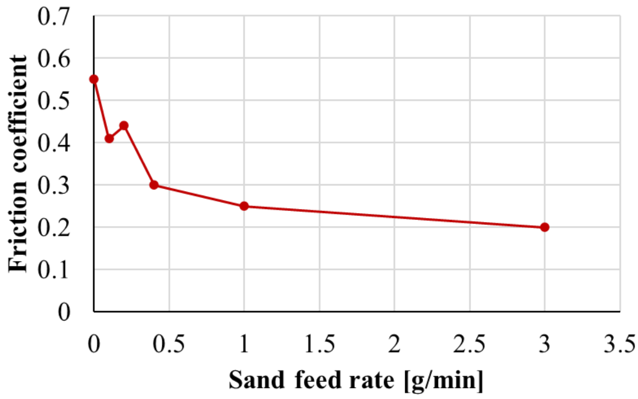

Figure 2 – Friction coefficients with respect to sand feed rate.

Figure 3 depicts the change in wear rate, measured as the amount of mass loss per unit distance, concerning the sand feed rate. There are two distinct phases observed. When the sand feed rate is below 0.4 g/min, there is a transient pattern characterised by an increase in the wear rate of the wheel and a decrease in the wear rate of the rail. On the other hand, when the sand feed rate equals or exceeds 0.4 g/min, the wheel wear rate begins to decline, while the rail wear rate starts to rise, eventually reaching a stabilised level. This change in behaviour at higher feed rates can be attributed to sand particles embedded in the wheel sample and to abrasion on the surface of the rail.

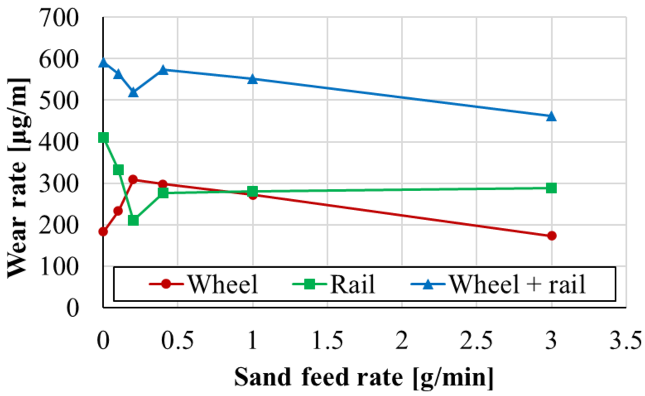

Figure 3 – Wear rate as a function of sand feed rate.

3.2. Surface damage and roughness

Figure 4 shows the surface roughness of worn wheel and rail specimens respect to sand feed rate. Both the surface roughness of rail and wheel kept relatively stable between 0 and 0.4 g/min, and subsequently presented a sharply increasing trend. It also indicated that the sand feed rate of 0.4 g/min was a critical point when the sand started to affect the surface roughness of wheel and rail evidently. Furthermore, the surface roughness of wheel was also very close to that of rail.

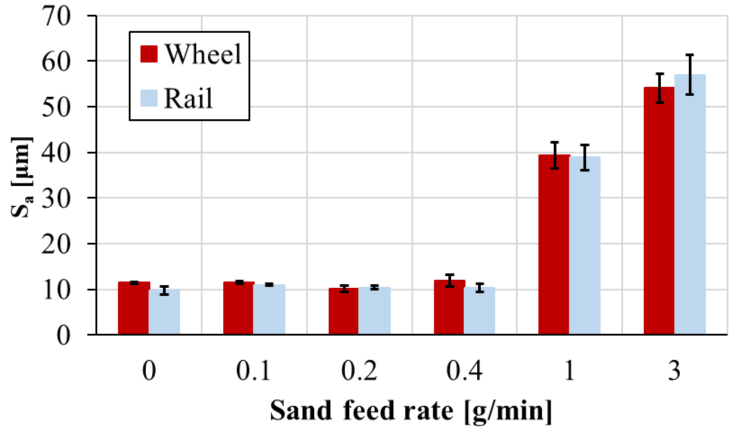

Figure 4 – Arithmetical mean height S_a as a function sand feed rate for wheel and rail samples.

Figure 5 illustrates the macroscopic damage patterns on the wheel surface under varying sand feed rates. Specifically, in Figure 4a, it's noticeable that when the sand feed rate was below 0.1 g/min, the predominant surface damage feature on the wheel was clearly fatigue cracks. However, as the sand feed rate increased, the prominence of fatigue cracks diminished, giving way to the formation of grooves. To gain insight into the dimensions of these macroscopic damage patterns, a three-dimensional profile of the surface morphology was measured and is presented in Figure 6. The data reveal a clear trend: as the sand feed rate rose, both the depth and width of the grooves increased. Moreover, it became increasingly evident that the overall surface condition deteriorated with higher sand feed rates.

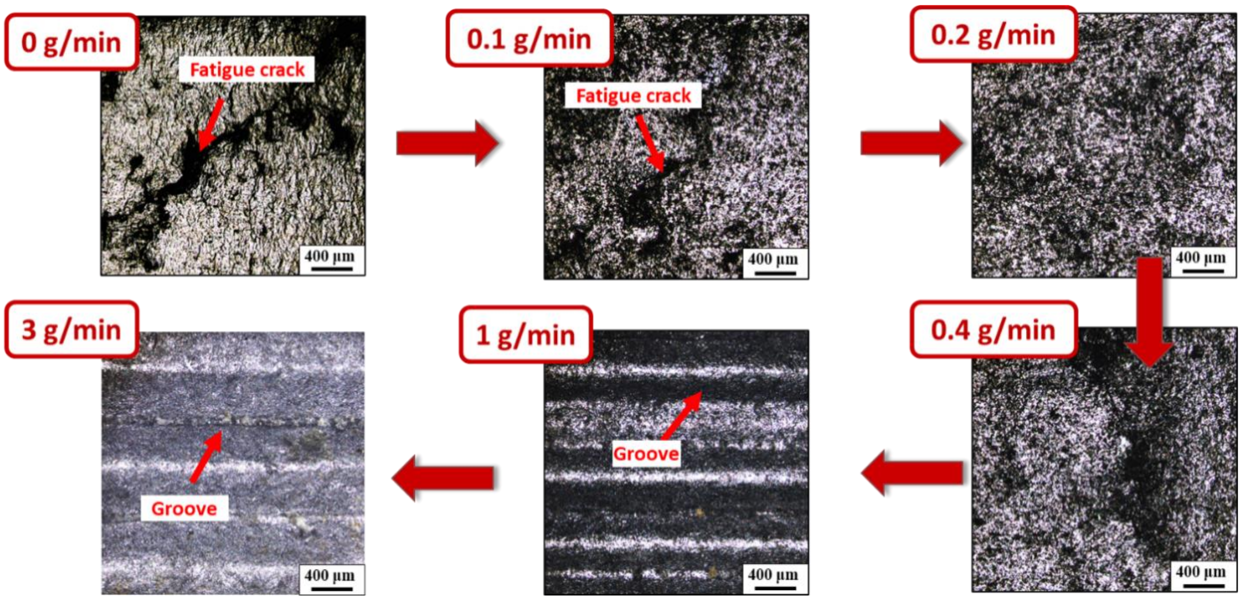

Figure 5 – Optical micrographs of the worn wheel surfaces.

Figure 7 displays the SEM images of the wheel surfaces after wear tests with three different sand feed rates (0, 0.2, 3 g/min). In Figure 6a, when no sand was introduced, aside from noticeable fatigue cracks, the wheel surface damage also featured clear furrows caused by abrasive wear from debris. Figures 7b and c illustrate that as the sand feed rate increased, the surface damage included not only fatigue cracks and furrows but also unevenly distributed oxides. Interestingly, the level of oxidation at the sand feed rate of 0.2 g/min was more severe than that at the sand feed rate of 3 g/min. This suggests that the oxidative wear of the wheel initially intensified and then diminished as the sand feed rate increased. Concurrently, fatigue wear decreased as the sand feed rate rose. Notably, abrasive wear was consistently present under all conditions.

Figure 8 shows the EDS analysis of worn wheel surfaces under three grades of sand feed rate (0, 0.2, 3 g/min). The elements Fe, O, and Si were detected on the worn wheel surfaces under all conditions. However, the proportion of these three elements varied significantly with different sand feed rates. The Si content on the worn wheel surfaces exhibited an upward trend as the sand feed rate increased. Additionally, it indicated that the quantity of sand remaining on the worn wheel surface increased with the rise in sand feed rate, which could potentially impact the measurement of the actual mass loss of the metal material.

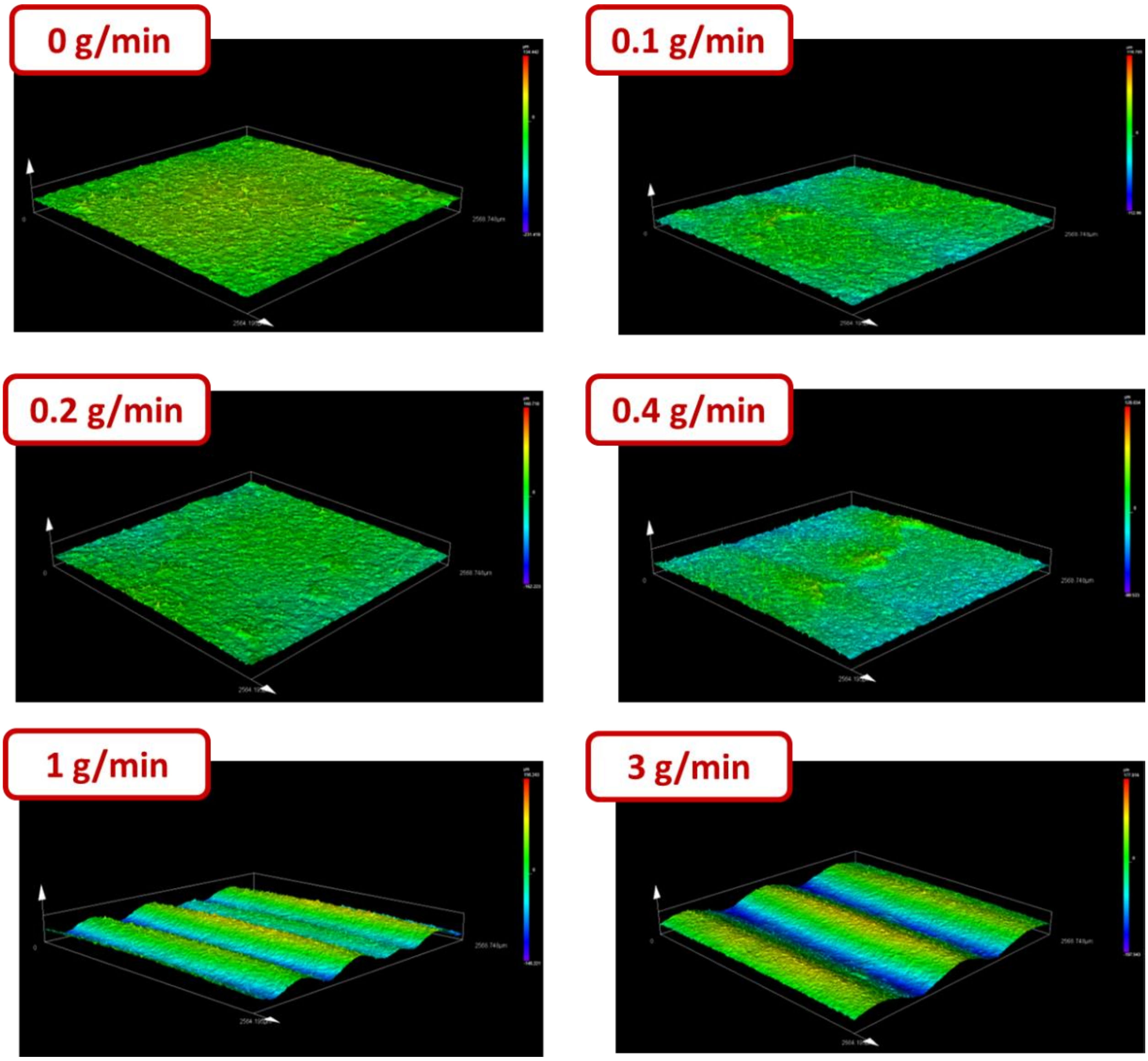

Figure 6 – Macroscopic damage morphology and three-dimensional profile of wheel surfaces with respect to sand feed rate.

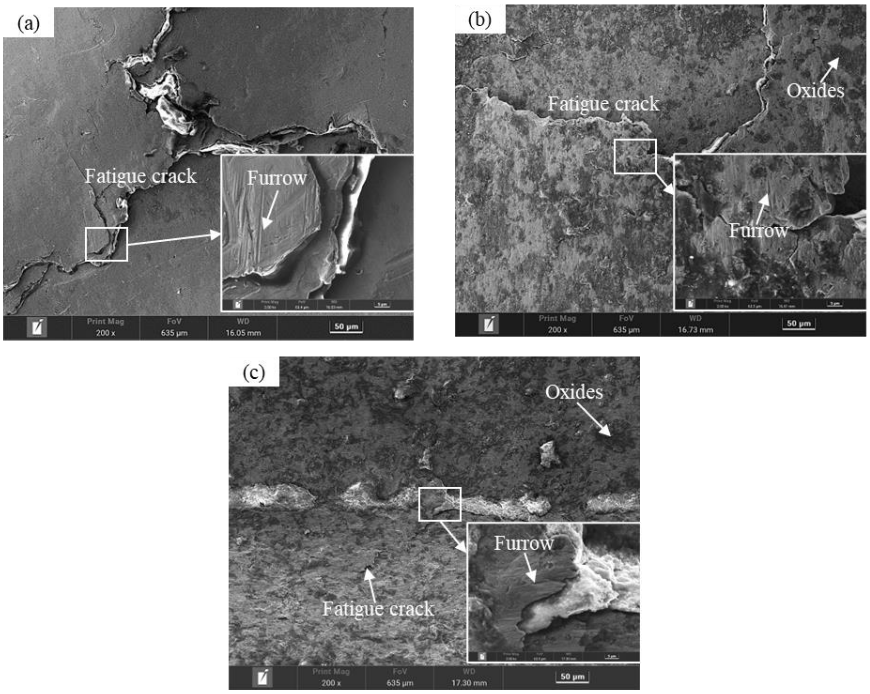

Figure 7 – SEM morphology of the wheel surfaces under different sand feed rates: (a) 0 g/min; (b) 0.2 g/min; (c) 3 g/min.

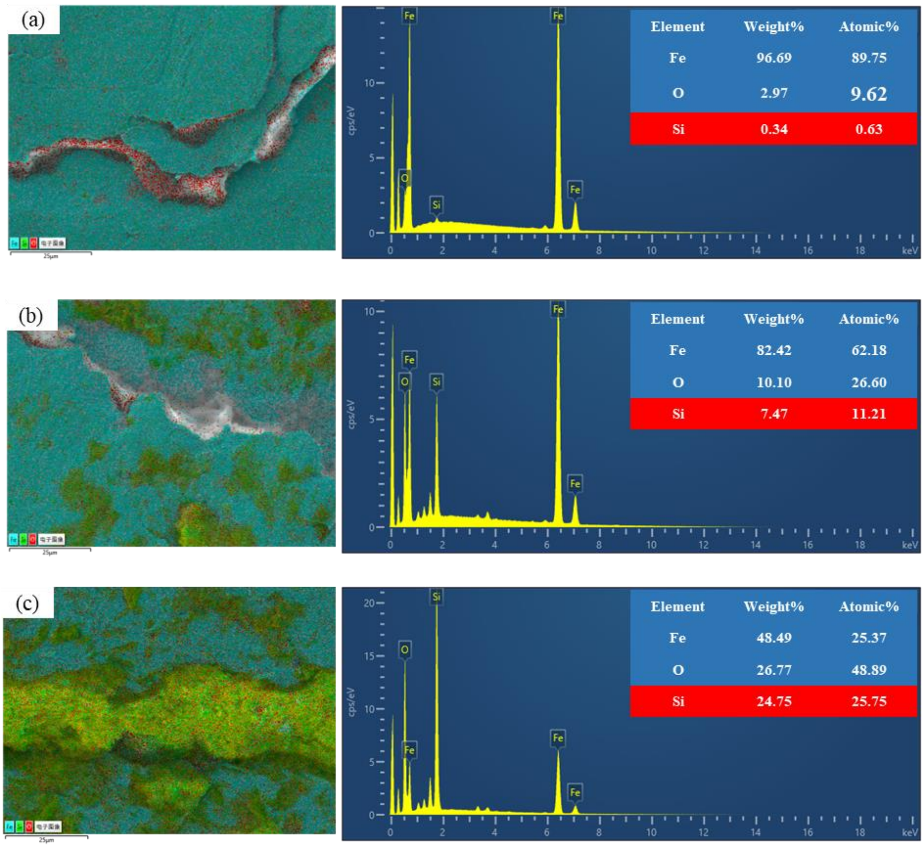

Figure 8 – EDS analysis of wheel surfaces under different sand feed rates: (a) 0 g/min; (b) 0.2 g/min; (c) 3 g/min.

3.3. Subsurface damage

When contact friction is present, the steel microstructure exhibits elongation along shear bands aligned with the friction direction. The plasticized depth is commonly defined as the distance from the surface to the point where the grains in the subsurface have not experienced deformation (see Figure 9). Figure 10 shows the depth of plasticisation in the wheel samples as it changes with varying sand feed rates. Up to 0.2 g/min, this parameter experiences a reduction. This finding could be somewhat deceptive if examined in isolation, as it suggests increased resistance to ratcheting when small amounts of sand are introduced into the contact area. However, it is worth noting that the wear rate increases under these conditions, leading to a reduction in deformed layer depth. When the feed rate exceeds 0.4 g/min, the depth of the plasticised layer increases, even though the wear rate decreases. This could be related to different wear damage phenomena when higher feed rates are applied: two distinct plastically deformed layers can be observed. The first is a surface layer exhibiting intense plastic flow and ratcheting caused by grooves resulting from wear debris and sand trapped inside the contact patch. The second is a deeper surface layer with less intense ratcheting. Figure 11 illustrates a cross-section of the sample tested at 3 g/min, with SEM-EDS analysis results showing crushed particles embedded in the surface disc.

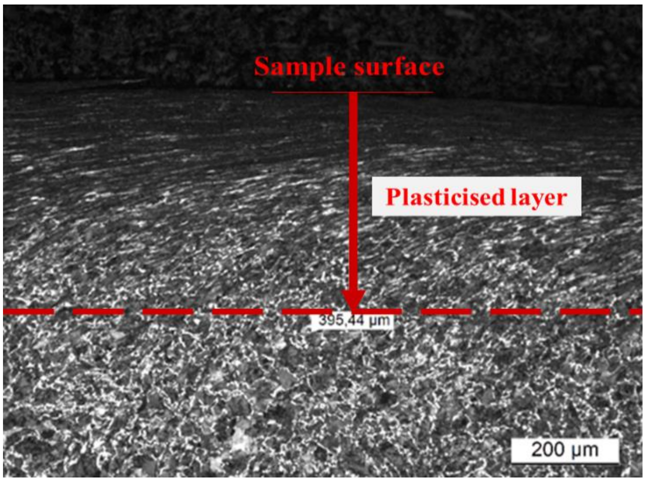

Figure 9 – Example of optical micrograph and detail of the plasticised layer (wheel sample, 0.2 g/min).

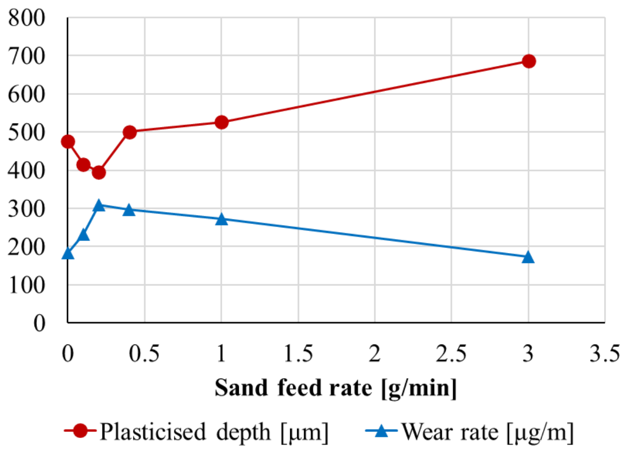

Figure 10 – Plasticised depth correlated to wear rate according to sand feed rate.

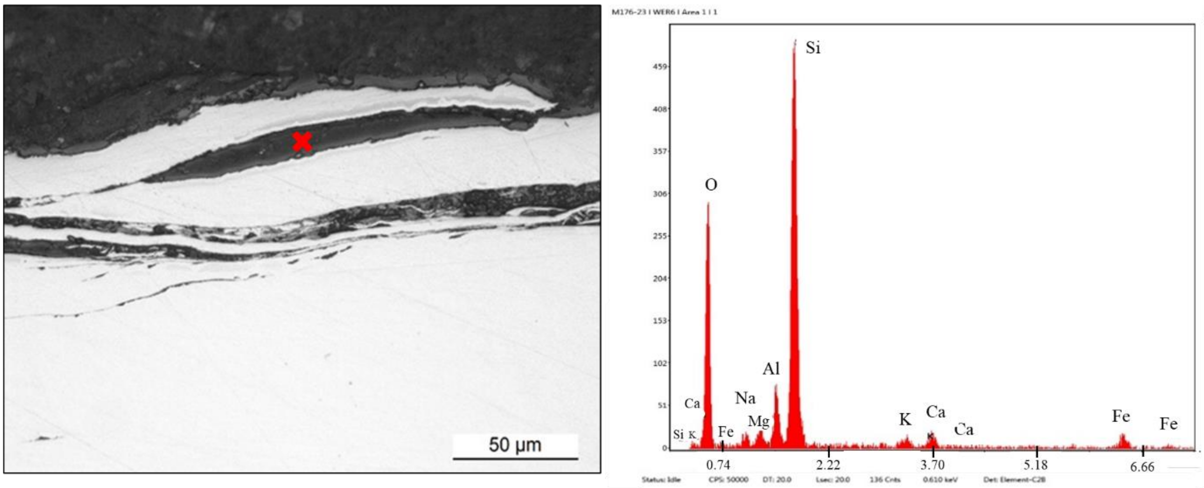

Figure 11 – On the left, optical micrograph of cross section wheel sample; on the right, EDS analysis of the material entrapped in the surface layer (ER8, 3 g/min).

4. Conclusions

The study examined the impact of sand feed rate on the damage and wear characteristics of railway wheel steel using bi-disc tests. Comparative tests were also conducted without sand. The study's findings lead to the following conclusions:

1. The friction coefficient displayed a consistent decreasing trend and reached an asymptotic value when the sand feed rate exceeded 1 g/min.
2. Fatigue wear was the main damage phenomenon in clean condition. Fatigue wear and oxidative wear were the primary wear mechanisms observed when the sand feed rate was less than 0.4 g/min. However, above this threshold, abrasive wear became the predominant mode of wear.
3. The oxide layers and the surface cracks contained randomly distributed sand particles.
4. Sand feed rates exceeding 0.4 g/min worsened surface damage on the samples, leading to the formation of grooves with increasing depth and width as the feed rate increased.
5. The plasticized depth exhibited a significant increase when the feed rate exceeded 0.4 g/min.

More work will be required to investigate whether these outcomes might be influenced by the sand particles granulometry and the geographical provenance of the sand.

References

[1] Arias-Cuevas O, Li Z and Lewis R 2011 A laboratory investigation on the influence of the particle size and slip during sanding on the adhesion and wear in the wheel-rail contact *Wear* **271** 14–24.
[2] Faccoli M, Petrogalli C, Lancini M, Ghidini A and Mazzù A 2018 Effect of desert sand on wear and rolling contact fatigue behaviour of various railway wheel steels *Wear* **396–397** 146–161.
[3] Wang W J, Lewis R, Yang B, Guo L C, Liu Q Y and Zhu M H 2016 Wear and damage transitions of wheel and rail materials under various contact conditions *Wear* **362–363** 146–152.
[4] Zani N and Petrogalli C 2022 Predictive maps for the rolling contact fatigue and wear interaction in railway wheel steels *Wear* **510–511** 204513.
[5] Gutsulyak D, Stanlake L J E and Qi H 2021 Twin Disc Evaluation of Third Body Materials in the Wheel / Rail Interface *Tribol. - Mater. Surfaces Interfaces* **15:2** 339–349.
[6] Shu K, Wang W, Ding H, Lin Q, Meli E, Guo J, Mazzù A and Liu Q 2022 Influence of sand transport rate on rolling wear and damage behaviors of wheel/rail in Gobi and desert windblown sand environments *Tribol. Int* **172** 107584.
[7] Gallardo-Hernandez E A and Lewis R 2008 Twin disc assessment of wheel/rail adhesion *Wear* **265:9–10** 1309–1316.

[8] Omasta M, Machatka M, Smejkal D, Hartl M and Křupka I 2015 Influence of sanding parameters on adhesion recovery in contaminated wheel–rail contact *Wear* **322–323** 218–225.
[9] Wang W J, Zhang H F , Wang H Y, Liu Q Y, and Zhu M H 2011 Study on the adhesion behavior of wheel/rail under oil, water and sanding conditions *Wear* **271**:**9–10** 2693–2698.
[10] Zani N, Chaise T, Ghidini A, Faccoli M and Mazzù A 2021 Numerical study about the effect of bainitic traces on plasticity in ferritic-pearlitic railway wheels *Proc. Institutions Mech. Eng. Part F J. Rail Rapid Transit* **235(6)** 726–740
[11] Grieve D G, Dwyer-Joyce R S, and Beynon J H 2001 Abrasive wear of railway track by solid contaminants *Proc. Inst. Mech. Eng. Part F J. Rail Rapid Transit* **215:3** 193–205.
[12] Mazzù A, Ghidini A, Zani N and Faccoli M 2021 A simplified numerical study of wheel/rail material coupling in presence of solid contaminants *Tribol. - Mater. Surfaces Interfaces* **15:2** 102–114.
[13] Mazzù A, Ghidini A, Zani N and Faccoli M 2018 Study of wheel/rail material coupling in presence of solid contaminants *Proc. 11th Int. Conf. Contact Mech. Wear Rail/wheel Syst (CM2018)* (Delft: the Netherlands) pp 701–710.
[14] Huang W, Cao X, Wen Z, Wang W, Liu Q, Zhu M and Jin X 2017 A Subscale Experimental Investigation on the Influence of Sanding on Adhesion and Rolling Contact Fatigue of Wheel/Rail under Water Condition *ASME J. Tribol*. **139:1** 011401.